Aerial Arch Bridge Construction

Precise and flexible assembly with drones using a 6dof parallel manipulator

Xingjie Xie[1], Xiaofan Gao[2], Menghao Yuan[3], Philip F. Yuan[4]*
[1,2,3,4]Tongji University
[1,2,3,4]{starxie|2230080|lyleyuan|philip007}@tongji.edu.cn

Aerial robotic construction offers an innovative solution for sustainable development, enabling drones to operate in high-risk, hard-to-reach, and complex environments. While drones enhance efficiency and safety, achieving precision in high-accuracy assembly remains a challenge. This paper proposes a method integrating a 6-degree-of-freedom parallel manipulator with a quadrotor drone to improve flexibility and precision. The system compensates for position and attitude errors while precisely controlling the end-effector for aerial tasks. The proposed system features an electromagnet and force sensors for precise material handling. The software framework, based on Grasshopper and ROS, includes real-time control, NURBS trajectory planning, and position compensation algorithms. To validate its effectiveness, a prototype of a 2.7-meter-span arch bridge was constructed, demonstrating the feasibility of assembling non-horizontal components with aerial robots. This research marks a milestone by achieving precise aerial assembly of complex structures, overcoming traditional precision limitations. It lays a foundation for future applications, advancing the role of aerial robots in construction for safer, more efficient, and flexible operations.

Keywords: *Aerial Fabrication, Parallel Manipulator, Arch Structure, Precise, Flexible.*

INTRODUCTION

Aerial Robotic Construction is an emerging technology that uses drones or other aerial robots for constructing buildings or structures. First proposed in 2012, this method differs from traditional ground-based construction techniques by relying on flying devices to carry out various construction tasks, such as transporting, assembling, and installing building materials and components (Jan et al., 2012). This approach demonstrates significant advantages in hazardous environments, hard-to-reach places, and unknown environments (such as Mars), offering a substitute for manual labor, enhancing efficiency, and reducing personnel risks.

Aerial robotic construction is characterized by its flexibility and maneuverability, allowing free movement in three-dimensional space and enabling operations in areas that are difficult for traditional equipment to reach. This capability makes it possible for aerial robots to perform intricate structural installations and assemblies in high-altitude, sloped, or extreme environments. For instance, when constructing skyscrapers, bridges, and other high-altitude structures, drones can execute inspection, repair, and construction tasks without the need to erect scaffolding or use large cranes.

However, ensuring the operational precision of aerial robots for dynamic tasks requiring high accuracy, such as installation and assembly, poses a significant challenge. Overcoming these challenges is crucial to unleashing the full potential of drones in construction.

Figure 1
Aerial robot in installation operation

This paper introduces an innovative aerial robotic construction method based on a 6-DOF parallel arm. This approach aims to achieve flexible end-effector motion through real-time compensation and attitude control of the parallel manipulator, overcoming the limitations of traditional drone operations. Combining a parallel arm with a quadrotor drone provides a flexible solution for complex construction tasks.

In terms of hardware, this paper designs a quadrotor drone, a specially designed 6-DOF parallel manipulator, and a grasping tool head based on electromagnets and force sensors. On the software side, the method includes a real-time control framework based on Grasshopper and ROS, a pose compensation method based on the 6-DOF parallel arm, an end-effector control method based on a two-dimensional force sensor, and a path planning method based on NURBS (Non-uniform rational basis spline).

To validate the effectiveness of this method, a full-size arch bridge prototype composed of non-horizontal discrete units was designed (Figure 1). Through practical aerial construction experiments, the feasibility and efficiency of the method were demonstrated, highlighting its great potential in aerial construction. This research marks a significant milestone in the field, achieving the first aerial robot assembly of non-horizontal components and construction of an arched structure.

STATE OF THE ART

In the current field of architecture, the development of aerial robotics is rapidly fostering a revolutionary transformation. Since 2012, a series of research papers on aerial robotics in architecture have emerged, revealing the potential and application prospects of this technology in architectural design and construction.

The earliest research proposed and investigated a system for assembling 2.5-dimensional structures by a team of quadcopters (Quentin et al., 2012). This research demonstrated that any SCS (special cubic structure) could be constructed through feasible assembly patterns and provided simulation and experimental results

for automated assembly by quadrotor teams. Subsequently, research on drone assembly of foam towers directed our attention to the concept of Aerial Robotic Construction (ARC) (Jan et al., 2012). which involves using autonomous flying vehicles to lift and precisely position building elements according to digital blueprints. The dynamic assembly of a six-meter-high tower by autonomous quadrotor aircraft was demonstrated, showcasing both the immense potential and the challenges of ARC, despite being in its early stages.

Since then, research teams have further expanded on this concept, exploring the possibility of using quadcopter teams to construct tension structures, highlighting the potential of aerial robots in building complex structures (Mirjan et al., 2013). This research initially described a set of aerial construction commands for the aircraft, such as node assembly and link erection, and the topological relationships between the aircraft's trajectories and the ropes. It then explored the combination of these commands and their applications in architectural production.

However, in recent years, aerial robotics technology has truly reached a new height. The integration of cyber-physical macro-materials with aerial construction robots has enabled reconfigurable building systems, further enhancing the flexibility and adaptability of architectural design (Dylan et al., 2019). Research on aerial additive manufacturing has pushed the boundaries of aerial robotics technology even further, utilizing multiple autonomous robots for 3D printing and providing new possibilities for constructing structures in complex environments (Ketao et al., 2022).

Broadly speaking, current literature covers various applications of aerial robotics in construction, including foam tower building, 2.5D cubic structures, tensile structure bridges, multi-agent building materials, and aerial additive construction. However, existing literature still has limitations regarding the potential of aerial robots in terms of precision and flexibility, as well as their practical applications in complex environments. The uniqueness of this study lies in its pioneering introduction of an aerial robotic construction method based on a 6-DOF parallel manipulator. This method aims to address the challenges faced by traditional construction methods and validate its feasibility and superiority through actual aerial construction experiments, filling gaps in the existing literature and paving the way for future applications of aerial robotics in the field of architecture. The main contributions of this paper are as follows:

- Combining a 6-DOF parallel manipulator with a traditional quadrotor UAV for the first time, achieving flexible end-effector postures in the air.
- Using aerial robots to assemble a 2.7-meter span arch bridge made of irregular components for the first time.
- Developing a set of applicable hardware devices and software frameworks for the aforementioned tasks.

METHODOLOGY

We introduce our methodology primarily through the design of the robotic system, the parallel manipulator, and the end-effector.

Aerial Robotics System

The aerial robot mainly consists of four components: a traditional quadrotor aircraft, a 6-DOF manipulator arm, a tool head, and a landing gear (Figure 2). The aircraft has a wheelbase of 600mm and propeller diameter of 15 inches, making it a medium-sized UAV capable of safely carrying a total takeoff weight of up to 14kg, including the aircraft itself, the parallel arm, and any materials it needs to carry.

The onboard computer is an Intel NUC, serving as the brain of the entire onboard system, capable of running ROS and various key control nodes (Figure 3). It can connect to a wireless

router via WiFi to receive real-time control messages and positioning data from the ground computer. Additionally, it provides sufficient computational power to run SLAM algorithms for obstacle avoidance data for the UAV. The onboard computer is also connected to the flight controller (brain), the arm (6-DOF parallel arm), the hand (electromagnet), and the feet (landing gear). The electromagnet, force sensor, and landing gear are all controlled by an Arduino Nano.

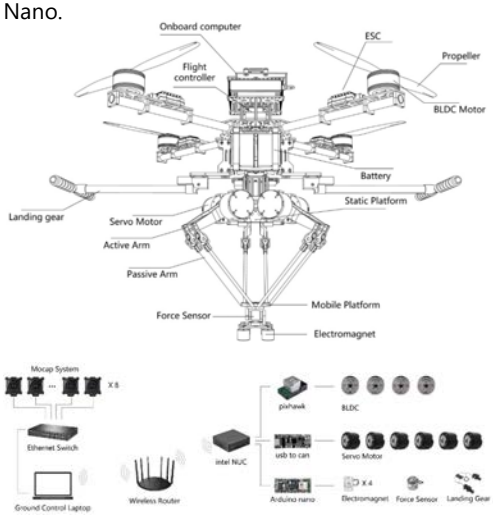

Figure 2
Components of the aerial robot

For positioning, this study employs an infrared motion capture system to provide real-time feedback on the spatial position and orientation of the UAV. Its absolute positioning accuracy is approximately 0.5mm, meeting the requirements for construction precision.

In terms of control, we utilize Grasshopper as the terminal tool to better obtain the position and orientation information of each block in parametric design. We have independently developed a set of Grasshopper components, including takeoff control, path and attitude transmission, path triggering, landing gear switch, emergency button, etc. Each component can send corresponding commands to the onboard computer by inputting the local IP of the onboard computer.

After obtaining the target position and orientation information of specific blocks, the system automatically generates multiple trajectories and desired end effector attitudes for the block, as well as allowable errors, etc. Each path contains a list of desired path points. This information is input into a Data Dam for path and attitude batteries. Once the battery receives new data, it sends it to the corresponding ROS node. In general, only triggering the takeoff and path grasshopper component is required for the drone to complete all operations automatically. The other three batteries are used for handling emergencies, allowing the drone to return to the takeoff and landing point automatically.

Regarding internal communication on the onboard side, we use the ROS robot operating system as the information channel between various nodes at the bottom layer to achieve effective information transmission and collaborative operation. This mainly includes takeoff control nodes, aircraft path control nodes, parallel arm control nodes, and Arduino control nodes.

Figure 3
Hardware system architecture

6-DOF Parallel Manipulator

In this section, we primarily introduce the origin of the 6-DOF Parallel Manipulator, along with its specific design and control.

Kinematic Model and Key Parameter. Traditional multi-rotor UAVs have 6 degrees of freedom; but when hovering, only 3 degrees of freedom of position remain. Therefore, to achieve 6 degrees of freedom in aerial construction, we use a 6-DOF parallel manipulator (Figure 4). The solution involves using a parallel manipulator with relatively lightweight rods, which do not significantly affect the aerial base's motion. This allows for compensation of the aerial base's position errors while achieving changes in the end effector's attitude.

A typical 6-DOF parallel manipulator consists of a static platform, a moving platform, six active arms, and six passive arms. Point A is a high-precision, high-torque servo motor; point B is a universal joint with 2 degrees of freedom; point C is a spherical joint with 3 degrees of freedom. The servo motor drives the active arm's motion, which in turn moves the passive arm's end position, thus changing the position and attitude of the moving platform, known as forward kinematics. To ensure that the workspace meets the requirements for position compensation and attitude changes, as well as to provide some additional space for further research, the design parameters are as follows: static platform radius Rs = 70mm, spacing Ls = Lm = 48mm, moving platform radius Rm = 22mm, active arm length Lp = 100mm, and passive arm length Ln = 180mm. The resulting workspace is shown as the gray area in the figure (Figure 4).

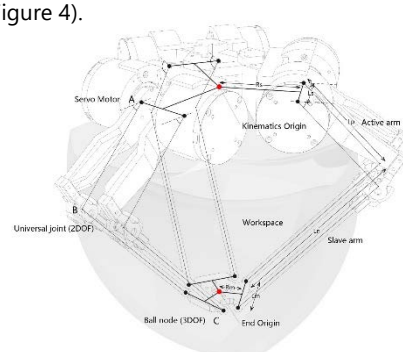

Figure 4
Kinematic model of the 6-dof parallel manipulator

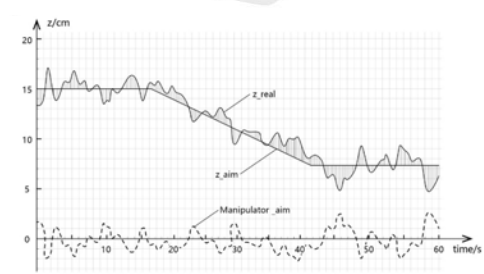

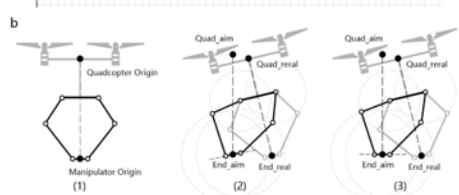

Figure 5
Real-time compensation:
(a) z-axis position compensation log
(b) real-time compensation in the presence of attitude error

Real-time Pose Compensation. For the previously designed medium-sized UAV, achieving high-precision position control is challenging due to its substantial weight. By adjusting the PID control parameters in the Position Controller and Attitude & Rate Controller, the system's precision limit can be approached, which is ±3cm (Figure 5-a).

During operation, taking height control along the Z-axis as an example, the data recorded over 60 seconds is shown (Figure 5-a). The z_aim is the UAV's desired value, but due to environmental factors and system errors, the actual value, z_real, exhibits discrepancies, represented by the shaded area. To eliminate this error, the difference between the two values can be used as the desired value for the parallel manipulator, Manipulator_aim, which is then input into its controller:

$$Manipulator\_aim = z\_aim - z\_real$$

However, the actual situation is far more complex since the aerial base always has some attitude error at any given moment. This means the problem is not simply a matter of addition and subtraction but involves rigid body transformations. Let's discuss real-time compensation. Figure 5-b-(1) shows a simplified model of the aerial robot, including the origin of the UAV body and the origin of the parallel manipulator's end-effector. The origin of the UAV body is defined as the Quadcopter Origin, whose position and attitude are obtained in real-time through the motion capture system. The origin of the manipulator, Manipulator Origin, is defined at the midpoint of its workspace to handle position errors from different directions. When planning the path, the Manipulator Origin should be directly below the Quadcopter Origin.

When there are position and attitude errors in the actual position and orientation of the aerial robot, the actual Quadcopter Origin, referred to as End_real, can be calculated through rigid body transformations. The desired Quadcopter Origin can then be used as the target value for the end-

effector. If only position errors need to be compensated, it corresponds to Figure 5-b-(2). If attitude errors also need to be compensated, ensuring the end-effector remains level, it corresponds to Figure 5-b-(3).

End Effector

Aerial construction, as a specialized building technique, imposes a series of unique requirements on the design of end-effectors: lightweight, electric-powered, rapid response, and reliability.

End Effector Calculation and Design. In response to these requirements, this study designed an electromagnetic-based end-effector (Figure 6). When the target object is a flat iron plate, four electromagnets can provide up to 24 kg of suction force. The electromagnets are powered by 24 volts and controlled via a MOS switch connected to an Arduino Nano. To equip the end-effector with a certain degree of sensing capability for better control decision-making, we also installed a force feedback device. This device has a range of ±2.5 kg, mapped to 0-1024, and is connected to the Arduino Nano through a transmitter.

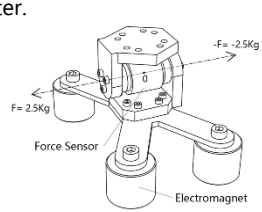

Figure 6
Design of the end effector

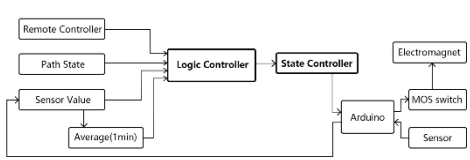

Figure 7
Control loop of the end effector

Control Based on Force Sensor. The control loop for the force sensor is as follows (Figure 7). The Arduino Nano receives real-time values from the force sensor at a frequency of 50 Hz and continuously sends these values to the ROS node Arduino_hub, while also recording the average value over the past minute. The Arduino_hub contains both a logic controller and a state controller.

The state controller communicates with the Arduino Nano, executing new commands only when there is a change in the instructions from the logic controller, thereby reducing communication bandwidth usage. The Arduino Nano then controls the MOS switch to toggle the electromagnet on or off.

AERIAL ASSEMBLY EXPERIMENTS

This section introduces the design of our arch bridge experiment and the key technical challenges involved.

Arch Bridge Design

To validate the novel construction method proposed in this paper, we designed a prototype of an arch bridge (Figure 8-a). The arch bridge spans 2.77 meters, with a height of 0.36 meters. The width narrows from 0.45 meters at the widest point to 0.25 meters at the narrowest point, from the sides towards the center. The bridge structure is symmetrical and consists of 17 components, displaying a gradient from cyan to magenta. The angle between the top surface of each component and the horizontal plane determines the angle the aerial robot's end-effector needs to maintain, with the maximum being 22.8° and the minimum being 0°.

Each component is constructed from six 4mm thick acrylic plates joined vertically. These plates are fastened together with bolts and nuts, with three parallel plates installed in the main load-bearing direction of the arch. The connecting sides of the components are equipped with four magnets for temporary fixation, attached to the acrylic plates via 3D-printed plastic connectors and bolts. The top surfaces of the acrylic plates feature four circular holes, with 3mm thick iron sheets mounted at the bottom of these holes to

allow the end-effector to accurately and securely pick up the components (Figure 8-b).

The side panels also have six pre-drilled holes for permanent fixation. Step 1 and step 2 demonstrate the temporary fixation using magnets, while step 3 shows the permanent fixation using bolts and nuts (Figure 8-c).

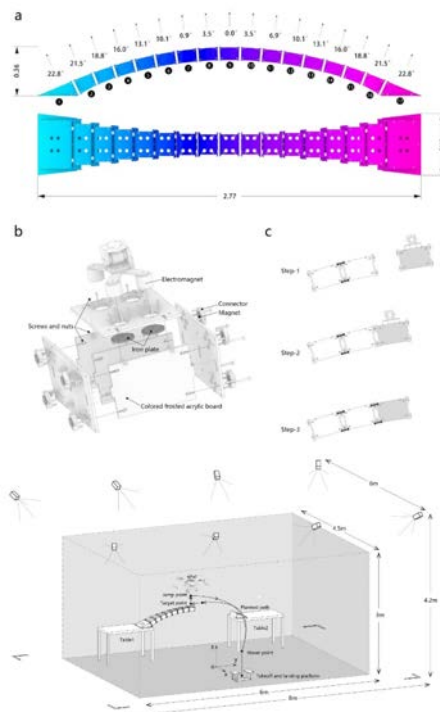

Figure 8
Arch bridge design: (a) arch bridge design diagram
(b) exploded view of modules
(c) permanent bolt installation.

Figure 9
Layout of the experimental site

Overall Workflow

We set up an experimental site measuring 8 meters in length, 6 meters in width, and 4.2 meters in height (Figure 9). The mocap cameras were evenly spaced and mounted at the top of the area. Two tables with lockable wheels are placed on the site to serve as the foundation for the bridge structure. A custom-made aluminum frame acts as the takeoff and landing platform, with a recessed area in the middle to place the bridge components.

The overall experimental procedure is as follows. First, lock the wheels of the tables to ensure stability. Fix the first component on the table using a large clamp, then sequentially install the remaining components using the aerial robot. Experiments showed that the magnetic nodes could support the weight of four components, but the magnet between the first and second components would detach when the fifth component was added. Once each component is secured with bolts, it remains fixed but may exhibit some deformation. Therefore, temporary support using tripods is applied every few components. Finally, connect the tables' bases with ropes, remove the supports, and unlock the tables' wheels.

The workflow for a single component is as follows. First, The robot is placed on the takeoff platform, and all software systems are initiated, ensuring that the onboard computer has received the path messages and motion capture data. Second, three motion capture markers are placed on the previously installed component, and this data is acquired in Grasshopper to calculate the current component's actual desired position and orientation. Third, the component is then manually attached to the end-effector. Last, by clicking the takeoff button in Grasshopper, the aerial robot autonomously completes the installation of the component and returns to the takeoff platform. The detailed assembly process for each component will be elaborated in the next section.

Path Planning and Projection Compensation

$P2^1$ and $P3^1$ represent the path of the aerial base, while all other path points are related to the end-effector (Figure 10). During the planning process, the desired position and orientation of the current component, P3, are first obtained. P3 is then translated 0.3 meters along its tangent to obtain P2.

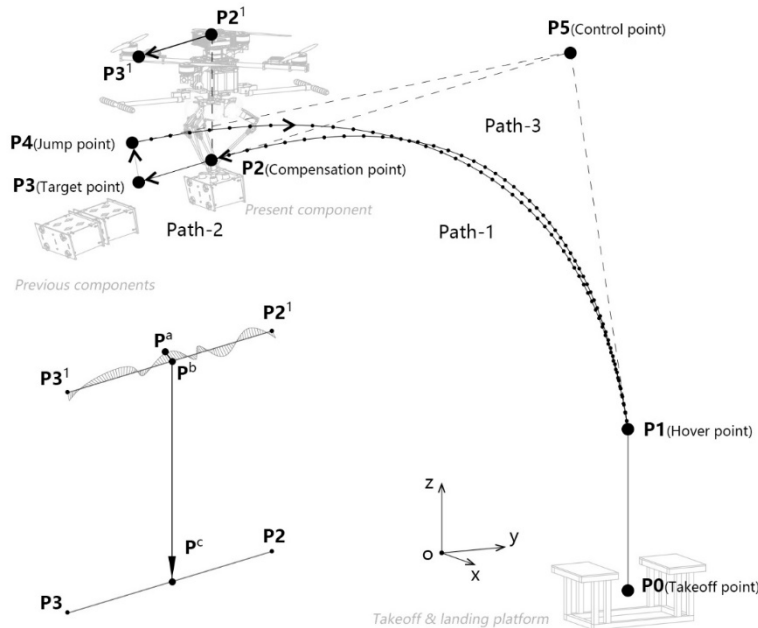

Figure 10
Path planning and projection compensation

and 0.15 meters along its normal to obtain P4. P2 is further translated 1.5 meters along the tangent to obtain P5. Consequently, path-1 is a NURBS curve with control points P1, P5, and P2; path-2 is a straight segment; and path-3 is another NURBS curve with control points P4, P5, and P1. All of these calculations are performed automatically in Grasshopper. The process is executed as follows:

1. Upon receiving the takeoff command, the aerial robot takes off from the platform to P1, folds its landing gear, and flies to P2 along path 1.
2. The parallel manipulator then compensates for the position errors of the aerial base and adjusts the end-effector to the required orientation for the component.
3. After successful compensation, the robot follows path 2, continuing real-time compensation until the installation is successful, indicated by a sudden change in the force sensor's value. At this moment, the electromagnet releases, and the end-effector returns to the origin of the parallel manipulator, with the aerial robot quickly flying upwards to P4.
4. Finally, the robot follows path 3 to return to P1 and automatically lands on the platform.

Special attention is needed for path 2, as it is a dynamic compensation process. $P2^1$ and $P3^1$ are the desired trajectories of the aerial base, but the actual path may deviate. The actual position, P^a, is projected onto the segment $P2^1P3^1$ to obtain P^b,

Figure 11
Aerial arch bridge assembly whole process

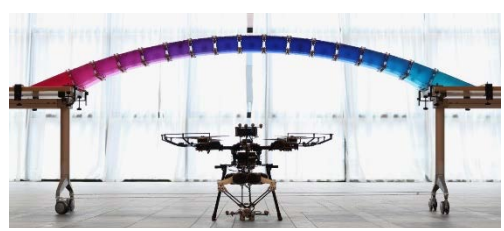

Figure 12
Aerial robot and completed arch bridge

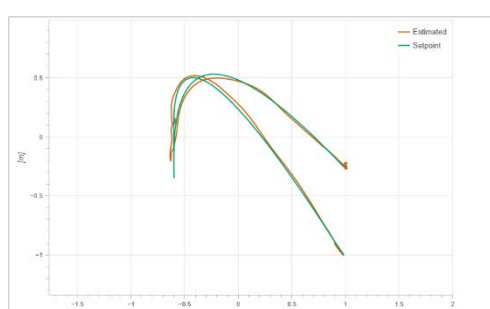

Figure 13
The trajectory of the aerial robot assembling one module

which is then further projected downward along the Z-axis to path 2, yielding P^c. P^c becomes the actual desired value for the end-effector. This precise sequence ensures that the aerial robot can adapt to dynamic conditions and accurately place the construction components, demonstrating the efficacy of the proposed method in real-world applications.

RESULTS AND DISCUSSION

The system's accuracy was assessed through a series of test flights and component installations. The results demonstrated that the aerial base could maintain a positional accuracy of ±3 cm during hover, as evidenced by the data recorded during the test flights (Figure 13). The parallel manipulator successfully compensated for this error, achieving a final installation accuracy within ±2 mm, well within the tolerances required for structural integrity.

The sequential installation process, leveraging the magnetic temporary fixation and bolted permanent fixation, proved effective. The average time taken to place and secure each component was approximately 1 minute, resulting in a total construction time of around 25 minutes (Figure 11, Figure 12).

Despite the successful experimental results, several challenges and limitations remain for practical application in real outdoor construction environments:

- Wind disturbances in outdoor settings increase installation errors, potentially requiring more advanced control algorithms.
- It may be necessary to design more robust connection methods and construction strategies between components to tolerate UAV-induced positioning errors.
- The integration of onboard LiDAR-based SLAM algorithms, RTK positioning, and total station-based tracking instead of mocap system could enhance system autonomy and adaptability to various environments.

Additionally, the 6-DOF parallel arm is currently limited to operating within tilt angles below 30°, which restricts the design of the arch bridge's rise height and inclination. In the future, alternative types of end-effectors could be considered to overcome this limitation in angular flexibility.

The demonstrated capability of the aerial robotic system to construct complex structures opens up numerous potential applications, from disaster relief construction to space habitat assembly. Future research will focus on improving the system's autonomy, expanding the range of compatible construction materials, and enhancing the robustness of the force feedback and control systems.

CONCLUSION

This paper proposes an aerial construction method based on a 6-DOF parallel robotic arm, aiming to address the challenges faced by traditional construction methods in complex and hazardous environments. By designing and implementing a medium-sized UAV, a 6-DOF parallel robotic arm, an electromagnetic end effector, and the associated software system, we have verified the feasibility and superiority of this method in practical applications.

However, this study also has certain limitations. Due to the limitations of the UAV's payload capacity and endurance, the application of the system in large-scale construction requires further exploration. Additionally, in practical applications, more adaptive modifications are needed for different building materials and structural forms.

ACKNOWLEDGEMENTS

This study was supported by the National Key R&D Program of China during the 14th Five-Year Plan period (Grant No. 2023YFC3806900). The final experiment of this study was conducted during the workshop at CAADRIA 2024.

REFERENCES

Cao, H., Li, Y., Liu, C. and Zhao, S. (2024) 'ESO-based robust and high-precision tracking control for aerial manipulation', *IEEE Transactions on Automation Science and Engineering*, 21(2), pp. 2139–2155.

Chermprayong, P., Zhang, K., Xiao, F. and Kovač, M. (2019) 'An integrated delta manipulator for aerial repair: A new aerial robotic system', *IEEE Robotics & Automation Magazine*, 26, pp. 54–66.

Lindsey, Q., Mellinger, D. and Kumar, V. (2012) 'Construction of cubic structures with quadrotor teams', in Durrant-Whyte, H., Roy, N. and Abbeel, P. (eds.) *Robotics: Science and Systems* VII. Los Angeles: RSS, pp. 177–184.

Menges, A. (2015) 'The new cyber-physical making in architecture: Computational construction', *Architectural Design*, 85, pp. 28–33.

Mirjan, A., Gramazio, F., Kohler, M., Augugliaro, F. and D'Andrea, R. (2013) 'Architectural fabrication of tensile structures with flying machines', in *Proceedings of the 2nd International Conference on Sustainable Intelligent Manufacturing*, Lisbon, Portugal, pp. 513–518.

Willmann, J., Augugliaro, F., Cadalbert, T., D'Andrea, R., Gramazio, F. and Kohler, M. (2012) 'Aerial robotic construction towards a new field of architectural research', *International Journal of Architectural Computing*, 10(3), pp. 439–459.

Wood, D., Yablonina, M., Aflalo, M., Chen, J., Tahanzadeh, B. and Menges, A. (2019) 'Cyber physical macro material as a UAV [re]configurable architectural system', in Willmann, J. et al. (eds.) *Robotic Fabrication in Architecture, Art and Design 2018*. Zurich: ROBARCH, pp. 320–335.

Zhang, K., Chermprayong, P., Xiao, F. et al. (2022) 'Aerial additive manufacturing with multiple autonomous robots', *Nature*, 609, pp. 709–717.